Multi-Modular Matrix Converter Topology applied to Distributed Generation Systems

S Toledo*, R Gregor*, M Rivera†, J Rodas*, D Gregor*, D Caballero*, F Gavilán* and E Maqueda*

**Laboratory of Power and Control Systems, Facultad de Ingeniería, Universidad Nacional de Asunción*

E-mail: {stoledo, rgregor, jrodas, dgregor, dcaballero, fgavilan, emaqueda}@ing.una.py

†*Department of Industrial Technologies, Universidad de Talca*

E-mail: marcoriv@utalca.cl

Keywords: Multi-modular matrix control, predictive current control, distributed generation systems.

Abstract

In this paper, a multi-modular matrix converter (MMC) topology as the power conversion core to interconnect a six-phase wind energy generator to the grid is proposed and analyzed theoretically. The proposed architecture is useful in distributed generation systems, where each module consists of a three-phase matrix converter topology. Furthermore, a model-based predictive control will be applied to the MMC in order to evaluate the dynamic performance in the design of current control. Finally, simulation results based on a MatLab/Simulink will be discussed in order to highlight the most relevant characteristic of the proposed MMC topology.

1 Introduction

In the last decades, several renewable energy sources (RES) such as: solar, micro-hydraulic and wind energy systems are being closely studied and harvested to fulfill the needs of electrical energy consumption [1]. In the field of RES, a very active research area is focused in the multiphase wind energy generator (MWEG) systems. In particular, MWEG with multiple three-phase windings are very convenient for wind turbine (WT) and several studies employing these topologies have been conducted recently [2]. The main reasons of multiphase choice for WT are the possibility to split the power and the current between a higher numbers of phases, allowing the per-phase inverter power rating reduction. Furthermore, this configuration guarantees WT working continuity, even in presence of phase and/or inverter faults. Hence, the use of multiphase electrical drives in WT should enable to increase the reliability, the working time, and consequently, the annual energy yield, determining a reduction in the maintenance cost. In MWEG, the six-phase wind energy generator (SpWEG) with two sets of three-phase stator windings spatially shifted by 30 electrical degrees and isolated neutral points is probably one of the most widely discussed topology with fully rated back-to-back converter system to interconnect the energy source to the electrical network (grid), focused on distributed generation (DG) [3]. Moreover, on DG systems the most widely used power electronic grid-connected converter (GCC) are the active front-end (AFE), cascaded multilevel converters and neutral-point-clamped (NPC) topologies [4]–[6]. GCC topologies must ensure an efficient active and reactive flux control with minimum current and voltage harmonic distortions besides ensuring proper synchronization with the distribution networks. To accomplish this, several control and modulation methods such as: pulse width modulation (PWM), space vector modulation (SVM), vector control, fuzzy control, model-based predictive control (MPC), etc., have been proposed [7]. Nowadays, most converters used for interconnect the energy sources to the grid used storage energy elements (i.e. capacitor banks) which provide weight, volume and failure possibilities to the GCC topologies.

Recent research efforts have been focused in the development of a flexible power interface based on a modular architecture capable to interconnecting different RES and load, including energy storage systems to the grid. These efforts converge in the multi-modular matrix converter (MMC) topologies whose the main feature is the ability to provide a three-phase sinusoidal voltages with variable amplitude and frequency using fully controlled bi-directional switches without the use of storage energies elements [8]. These characteristics makes plausible the use of MMC in applications where is required high power density and compact converters such as SpWEG systems, constituting an attractive alternative if it is compared with conventional converter topologies [9].

The main contribution of this paper comparing to previous works is focused on a theoretical performance analysis of a MMC combined with a SpWEG scheme in order to ensure an efficient current control from the generator side to the grid side. Each module of the MMC architecture are connected in cascade to the independent three-phase windings of the SpWEG. A predictive current control by using a MPC technique is used to predict the effects of future control actions in order to minimize a defined cost function. The proposed grid interconnection architecture is shown in Fig. 1.

The paper is organized as follows. Section 2 describes the six-phase induction generator model. Section 3 discusses the modeling of the system. Section 4 is focus to the control

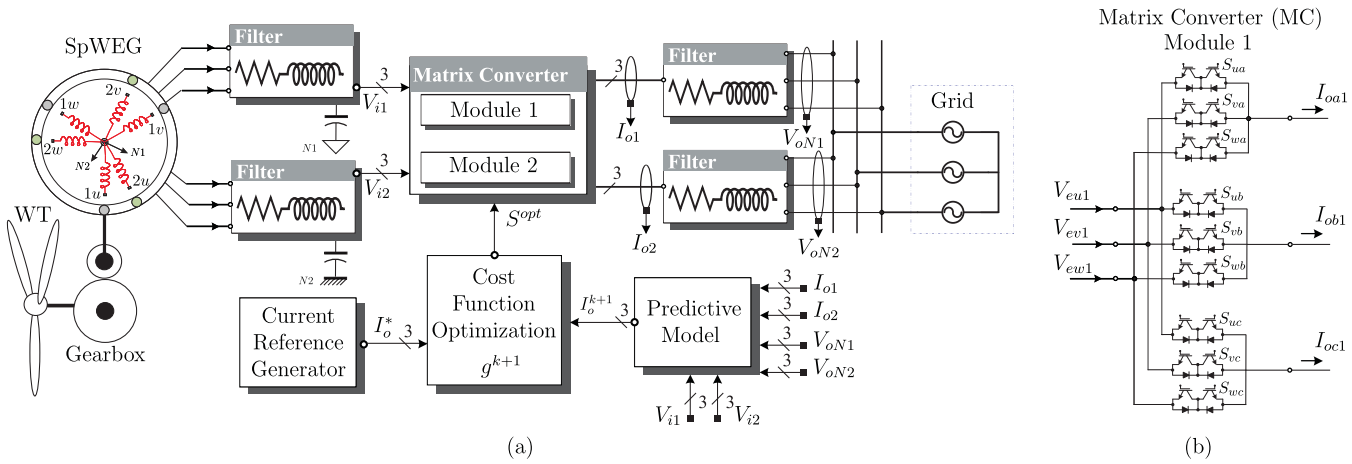

Fig. 1: (a) Proposed multi-modular matrix converter topology applied to the SpWEG. (b) Matrix converter topology.

strategy analysis and simulation results. Finally, concluding remarks are summarized in Section 5.

2 Generation system description

The power extracted from the wind can be modeled by the following equation [10]:

$$P_m = \frac{1}{2}\rho A \nu^3 C_p(\beta, \lambda), \tag{1}$$

where P_m represents the captured power (W); ρ the air density (kg/m^3); A the wind turbine swept area (m^2) and ν the wind speed (m/s). C_p represents the power coefficient of the wind turbine as function of the blade pitch angle β (degrees) and a dimensionless parameter λ which defines the relation between the rotational lineal speed of the turbine and the wind speed, as the following equation:

$$\lambda = \frac{R_t \omega_m}{\nu}, \tag{2}$$

where R_t and ω_m represents the turbine radius (m) and the turbine angular velocity (rad/s), respectively. It is noticeable that, if we want to maximize the captured power, it should be maintained C_p in its maximum value. A numerical approximation of the power coefficient for the wind turbine is given by the following equation:

$$C_p(\beta, \lambda) = 0.73\left(\frac{151}{\lambda_1} - 0.58\beta - 0.002\beta^{2.14} - 13.2\right) e^{\frac{18.4}{\lambda_1}}, \tag{3}$$

where $\lambda_1 = \left(\frac{1}{\lambda - 0.02\beta} - \frac{0.003}{\beta^3+1}\right)^{-1}$. Fig. 2 shows an estimate of the generated power as function of the turbine angular velocity for different wind speed values, derived by using a Matlab/Simulink simulation environment. The curve defines the maximum generated power as function of the optimal value of the turbine mechanical speed, which is the generator's rotor speed.

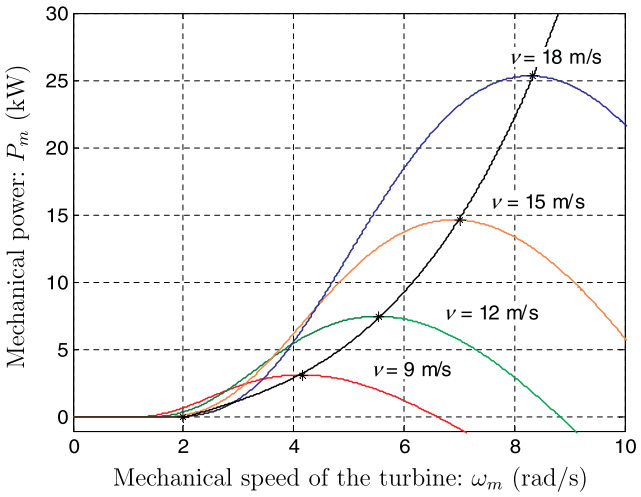

Fig. 2: Optimum captured power.

2. 1 Mathematical model of the SpWEG

The mathematical model of the SpWEG is very similar to the six-phase induction motor model, with differences in the SpWEG has a capacitor bank connected to its stator terminals, which must be considered in the model of the generator, and in this case, rotor speed, provided by the turbine is considered as input, and not output as the motor case. The analysis and control of the SpWEG using the vector space decomposition (VSD) approach is greatly simplified, since the generator model in $(\alpha - \beta)$ sub-space is identical to the model of the three-phase generator, Fig. 3.

If two stator set have isolated neutral points, it can be demonstrated that no currents components flows in the $(z_1 - z_2)$ sub-space. For this reason, the generator model referred to the stationary reference frame can be reduced to two sets of decoupled equations corresponding to the generator $(\alpha - \beta)$ and $(x - y)$ sub-space [11].

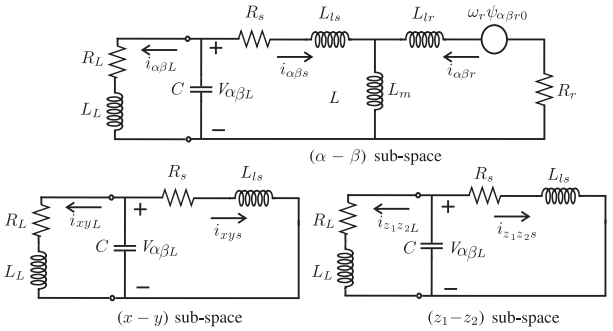

Fig. 3: Equivalent circuit of the SpWEG.

The mathematical model of the SpWEG can be written using the state-space representation form:

$$[\mathbf{G}]\frac{d}{dt}[\mathbf{x}]_{\alpha\beta}+[\mathbf{F}][\mathbf{x}]_{\alpha\beta}+[\mathbf{u}]_{\alpha\beta}=0, \tag{4}$$

where $[\mathbf{u}]_{\alpha\beta}=\begin{bmatrix} V_{\alpha C} & V_{\beta C} & \omega_r\psi_{\beta r0} & -\omega_r\psi_{\alpha r0}\end{bmatrix}^T$ denotes the generated voltage, $V_{\alpha\beta C}$ the capacitor voltage, $\psi_{\alpha\beta r0}$ the initial rotor flux, ω_r is the wind turbine rotor angular speed, $[\mathbf{x}]_{\alpha\beta}=\begin{bmatrix} i_{\alpha s} & i_{\beta s} & i_{\alpha r} & i_{\beta r}\end{bmatrix}^T$ represents the generator current, $[\mathbf{F}]$ and $[\mathbf{G}]$ are matrices that define the dynamics of the drive that for the particular case of the SpWEG are represented as follows:

$$[\mathbf{F}]=\begin{bmatrix} R_s & 0 & 0 & 0\\ 0 & R_s & 0 & 0\\ 0 & \omega_r L_m & R_r & \omega_r L_r\\ -\omega_r L_m & 0 & -\omega_r L_r & R_r\end{bmatrix}, \tag{5}$$

$$[\mathbf{G}]=\begin{bmatrix} L_s & 0 & L_m & 0\\ 0 & L_s & 0 & L_m\\ L_m & 0 & L_r & 0\\ 0 & L_m & 0 & L_r\end{bmatrix}, \tag{6}$$

where R_s and R_r are the stator and rotor resistance, $L_s=L_{ls}+L_m$, $L_r=L_{lr}+L_m$ and L_m are the stator, rotor and magnetizing inductances, respectively. For a generator with P pairs of poles, the electromagnetic generated torque (T_G) can be modeled by the following equation:

$$T_G=3\frac{P}{2}L_m\left(i_{\alpha s}i_{\beta r}-i_{\beta s}i_{\alpha r}\right). \tag{7}$$

The relationship between torque and rotor speed can be written as:

$$J_i\frac{d}{dt}\omega_r+B_i\omega_r=\frac{P}{2}\left(T_G-T_L\right), \tag{8}$$

being J_i the inertia, B_i the friction coefficient and T_L the load torque. The equations in $(x-y)$ sub-space do not link to the rotor side and consequently do not contribute to the air-gap flux, however, they are an important source of Joule losses. Using the state-space representation, these equations can be written as:

$$[\mathbf{u}]_{xy}=\begin{bmatrix} L_{ls} & 0\\ 0 & L_{ls}\end{bmatrix}\frac{d}{dt}[\mathbf{i}]_{xy}+\begin{bmatrix} R_s & 0\\ 0 & R_s\end{bmatrix}[\mathbf{i}]_{xy}, \tag{9}$$

being L_{ls} the stator leakage inductance. Assuming the mathematical model expressed by (4) and using the state variables defined by the vector $[\mathbf{x}]_{\alpha\beta}$, it can be defined as follows:

$$\begin{aligned}
\dot{x_1} &= c_3\left(R_r x_3+\omega_r x_4 L_r+\omega_r x_2 L_m+\omega_r\psi_{\beta r0}\right)+\\
&\quad c_2\left(-V_{\alpha C}-R_s x_1\right),\\
\dot{x_2} &= c_3\left(R_r x_4-\omega_r x_3 L_r-\omega_r x_1 L_m-\omega_r\psi_{\alpha r0}\right)+\\
&\quad c_2\left(-V_{\beta C}-R_s x_2\right),\\
\dot{x_3} &= c_4\left(-R_r x_3-\omega_r x_4 L_r-\omega_r x_2 L_m-\omega_r\psi_{\beta r0}\right)+\\
&\quad c_3\left(V_{\alpha C}+R_s x_1\right),\\
\dot{x_4} &= c_4\left(-R_r x_4+\omega_r x_3 L_r+\omega_r x_1 L_m+\omega_r\psi_{\alpha r0}\right)+\\
&\quad c_3\left(-V_{\beta C}+R_s x_2\right),
\end{aligned} \tag{10}$$

where c_i $(i=1,2,3,4)$ are constants defined as:

$$c_1=L_sL_r-L_m^2,\ c_2=\frac{L_r}{c_1},\ c_3=\frac{L_m}{c_1},\ c_4=\frac{L_s}{c_1}. \tag{11}$$

This set of differential equations are also used for the applied load conditions of the SpWEG. For an inductive load (RL) the components of differential load voltage equations can be written as:

$$\begin{aligned}
\frac{dV_{\alpha L}}{dt} &= \frac{1}{C}i_{\alpha C},\\
\frac{dV_{\beta L}}{dt} &= \frac{1}{C}i_{\beta C},
\end{aligned} \tag{12}$$

where $i_{\alpha C}=i_{\alpha s}-i_{\alpha L}$ and $i_{\beta C}=i_{\beta s}-i_{\beta L}$. The components of differential load current equations can be written as:

$$\begin{aligned}
\frac{di_{\alpha L}}{dt} &= \frac{1}{L_L}\left(V_{\alpha L}-R_L i_{\alpha L}\right),\\
\frac{di_{\beta L}}{dt} &= \frac{1}{L_L}\left(V_{\beta L}-R_L i_{\beta L}\right).
\end{aligned} \tag{13}$$

2. 2 Magnetizing inductance and capacitor of self-excitation

Although self-excitation does not occur during normal grid-connected operation, it can occur during off-grid operation. Under these operating conditions, the magnetizing inductance and stator magnetizing current cannot be considered constant. In these work, the relationship between the magnetizing inductance and magnetizing current is obtained experimentally from open-circuit test at synchronous speed with induction motor parameters listed in Table 1. The magnetizing inductance curves as function of magnetizing current is given in Fig. 4 and it is a nonlinear function of magnetizing current, which can be represented by a second order polynominal curve fit as:

$$\begin{aligned}
L_m &= -0.0213\,I_m^2+0.0631\,I_m+0.1774,\\
&\quad 0<I_m<2.9\ \text{A},
\end{aligned} \tag{14}$$

when the measured magnetizing current is:

$$I_m=\sqrt{\left(i_{\alpha s}+i_{\alpha r}\right)^2+\left(i_{\beta s}i_{\beta r}\right)}. \tag{15}$$

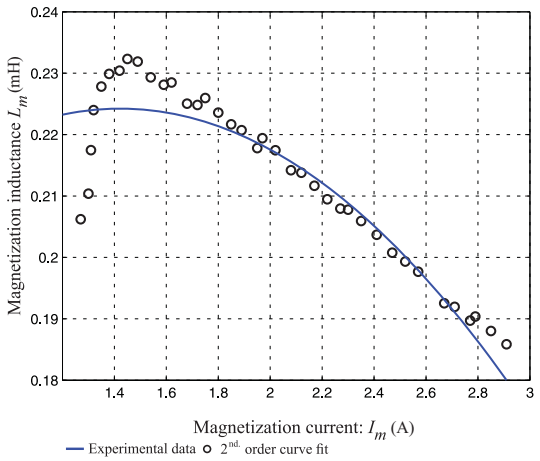

Fig. 4. Magnetizing inductance variation with the magnetizing current.

	Six-phase wind energy generator		
Parameter	Symbol	Value	Unit
Stator resistance	R_s	0.62	Ω
Rotor resistance	R_r	0.63	Ω
Stator inductance	L_s	0.2062	H
Rotor inductance	L_r	0.2033	H
System inertia	J_i	0.27	kg·m^2
Viscous friction coefficient	B_i	0.012	kg·m^2/s
Nominal frequency	f_a	50	Hz
Load torque	T_L	0	N·m
Number of pole pairs	P	3	–

Table 1: Electrical and mechanical parameters.

From Fig. 4, the design of capacitor bank of the self-excited SpWEG needed to generate the rated voltage under off-grid and rated speed conditions, the capacitance of the capacitor bank is defined as follows:

$$C_{min} = \frac{1}{\omega^2 L_m}. \tag{16}$$

By substituting (14) into (16), the minimum capacitance for build-up voltage at the rated speed under off-grid operation is $C_{min} \approx 51\mu$F, when the unsaturated magnetizing inductance is $L_m = 0.1998$ mH at the rated speed of $\omega_r = 1\,000$ rpm.

3 Model of the power conversion system

As it was shown in Fig. 1, the proposed topology consists of two three-phase matrix converter (MC) modules connected to the SpWEG by using a passive (LC) input filter and then connected to the grid by an output filter. Each one of these modules is represented by the power electronic scheme of the Fig. 5.

In this case, generated voltages by the SpWEG are indicated as V_{uj}, V_{vj} and V_{wj} where $j \in \{1, 2\}$ depending of the corresponding module. In the same way, the generated currents are indicated as I_{uj}, I_{vj} and I_{wj}. The output currents of the input filter are indicated as I_{eu}, I_{ev} and I_{ew}, respectively. Input voltages of the MC are V_{euj}, V_{evj}

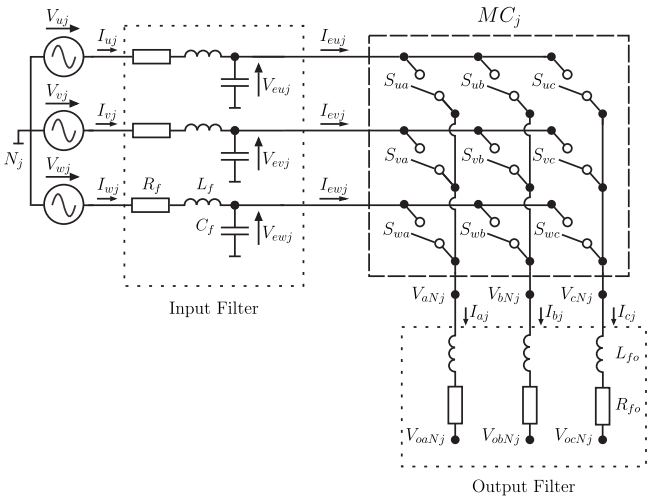

Fig. 5: Model of the power systems.

and V_{ewj}. The output voltages of the MC respect to the corresponding SpWEG neutral point (N_1 or N_2) are V_{aNj}, V_{bNj} and V_{cNj}. Moreover, output currents are I_{oaj}, I_{obj} and I_{ocj}, respectively. Finally, the output filter voltages (that are connected to the grid) are V_{oaNj}, V_{obNj} and V_{ocNj}.

The MC power topology is composed of nine bidirectional power switches, which can generate 27 feasible switching states [12]. If the three-phase vectors of voltages and currents are defined as:

$$V_{sj} = \begin{bmatrix} V_{uj} \\ V_{vj} \\ V_{wj} \end{bmatrix}, \quad V_{ij} = \begin{bmatrix} V_{euj} \\ V_{evj} \\ V_{ewj} \end{bmatrix}, \quad V_{oj} = \begin{bmatrix} V_{aNj} \\ V_{bNj} \\ V_{cNj} \end{bmatrix}$$
$$I_{sj} = \begin{bmatrix} I_{uj} \\ I_{vj} \\ I_{wj} \end{bmatrix}, \quad I_{ij} = \begin{bmatrix} I_{euj} \\ I_{evj} \\ I_{ewj} \end{bmatrix}, \quad I_{oj} = \begin{bmatrix} I_{oaj} \\ I_{obj} \\ I_{ocj} \end{bmatrix},$$

then the following vectorial equations relate the input and output voltages or currents in terms of the switching states of the MC:

$$V_{oj} = S \cdot V_{ij}, \qquad I_{ij} = S^T \cdot I_{oj}, \tag{17}$$

being S the instantaneous transfer matrix, defined as:

$$S = \begin{bmatrix} S_{ua} & S_{ub} & S_{uc} \\ S_{va} & S_{vb} & S_{vc} \\ S_{wa} & S_{wb} & S_{wc} \end{bmatrix}, \tag{18}$$

where the S_{xy} element has a binary value, corresponding to the state of the single switch.

In order to avoid short circuits on the input side and ensure an uninterrupted current flow on the load side, the switching signals S_{xy} must satisfy the following condition:

$$S_{uy} + S_{vy} + S_{wy} = 1, \quad \forall x \in \{a, b, c\}. \tag{19}$$

The dynamic model of the passive output filter is defined as:

$$V_{oj} - V_{oNj} = L_{fo}\frac{dI_{oj}}{dt} + R_{fo}I_{oj}, \tag{20}$$

where:

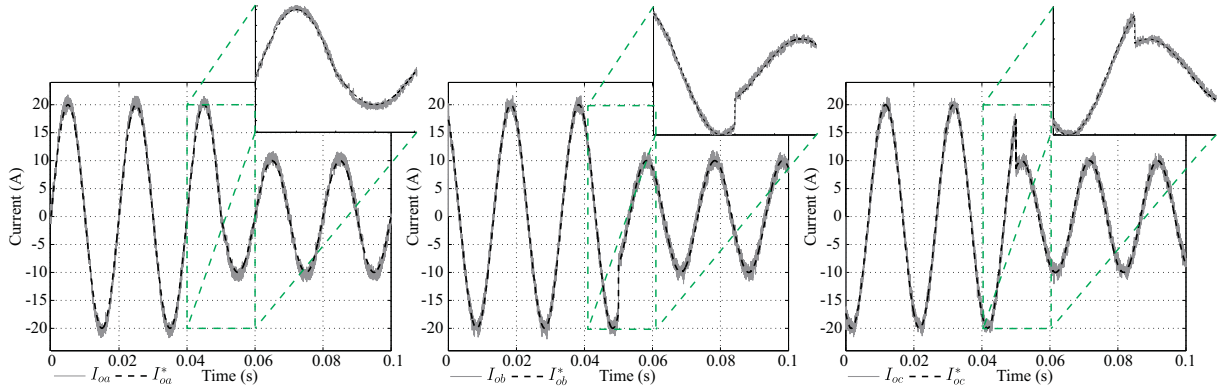

Fig. 6: Simulation results of the proposed strategy for amplitude changes.

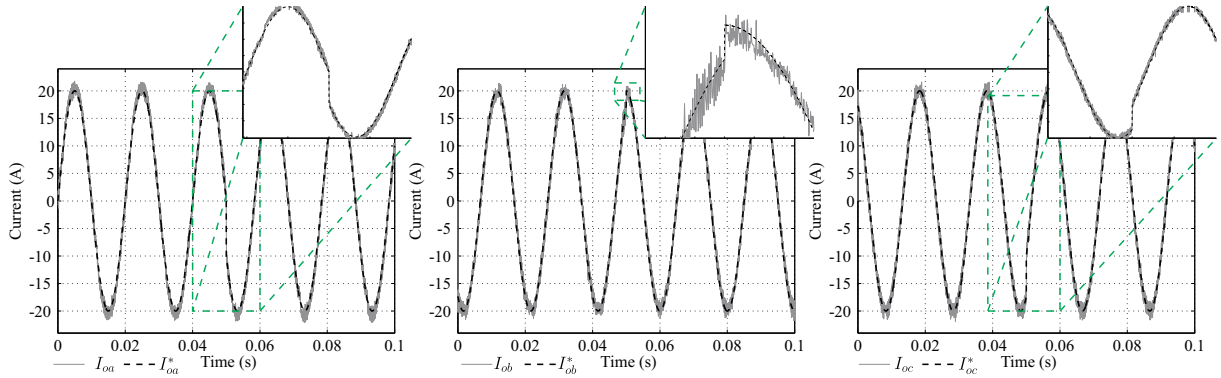

Fig. 7: Simulation results of the proposed strategy for phase changes.

$$V_{oNj} = \begin{bmatrix} V_{oaNj} \\ V_{ocNj} \\ V_{ocNj} \end{bmatrix}, \tag{21}$$

is the voltage vector measured from the end of the output filter to the corresponding neutral point N_j of the SpWEG. In the case of the input filter, the dynamic behavior can be directly modeled by using the space-state representation approach as:

$$\frac{d}{dt}\begin{bmatrix} V_{ij} \\ I_{sj} \end{bmatrix} = A_c \begin{bmatrix} V_{ij} \\ I_{sj} \end{bmatrix} + B_c \begin{bmatrix} V_{sj} \\ I_{ij} \end{bmatrix}, \tag{22}$$

where:

$$A_c = \begin{bmatrix} 0 & \frac{1}{C_f} \\ -\frac{1}{L_f} & -\frac{R_f}{L_f} \end{bmatrix}, \qquad B_c = \begin{bmatrix} 0 & -\frac{1}{C_f} \\ \frac{1}{L_f} & 0 \end{bmatrix}, \tag{23}$$

being L_f and C_f the filter inductance and capacitance, respectively, and R_f is the leakage resistance of L_f.

4 Control strategy and performance analysis

In this paper, an MPC technique for current control is implemented to control the current provided by a six-phase generator to the grid. The MPC technique uses a model of the system to predict the future behavior of the variables to be controlled. The inherent discrete nature of power converters simplifies the MPC optimization algorithm to the prediction of the system behavior only for the set of feasible switching states. This approach is called finite control set MPC, and it has been successfully used in several power converter applications and typologies [8], [9]. The discrete model of the system is derived from the continuous time linear system for the input filter, the output filter, and the $(\alpha-\beta)$ transform defined in [12] as:

$$\begin{aligned} x_\alpha &= \frac{2}{3}\left(x_a - 0.5x_b - 0.5x_c\right), \\ x_\beta &= \frac{2}{3}\left(\frac{\sqrt{3}}{2}x_b + \frac{\sqrt{3}}{2}x_c\right). \end{aligned} \tag{24}$$

The load current prediction, using the forward Euler discretization of (20), is

$$I_{oj}(k+1) = \left(1 - \frac{R_{fo}T_s}{L_{fo}}\right) I_{oj}(k) + \frac{T_s}{L_{fo}}\left(V_{oj}(k) - V_{oNj}(k)\right), \tag{25}$$

where T_s is the sampling time, $I_{oj}(k)$ and $V_{oNj}(k)$ are measured, and $V_{oj}(k)$ is calculated for all switch combinations to predict the next value of the output currents and evaluate the cost function in order to select the optimum solution.

In this case, the control criterion is the regulation of current supplied from the SpWEG to the grid. With this criterion, we propose to control every current of MC modules in such a way that they will be in phase at the point of connection and the resulting current will be the sum of all module currents. Thereafter, the reference currents for each modules

Parameter	Simulation parameters		
	Symbol	Value	Unit
Grid phase peak voltage	V_s	310	V
Grid frequency	f_s	50	Hz
Source line-to-line peak voltage	V_{uvw}	540	V
Source voltage frequency	f_{uvw}	50	Hz
Input filter leakage resistance	R_f	0.5	Ω
Input filter inductance	L_f	400	μH
Input filter capacitance	C_f	25	μF
Output filter resistance	R_{fo}	0.09	Ω
Output filter inductance	L_{fo}	30	mH
Sampling period	T_s	10	μs

Table 2: System and controller parameters.

are defined as half of the desired total currents as:

$$I^*_{oxj} = \frac{I^*_{ox}}{2},\ x \in \{a, b, c\}, \tag{26}$$

where I_{ox} represent the total current supplied in the x phase and I^*_{ox} is the reference current.

Using (24) we can calculate all currents in $(\alpha - \beta)$ subspace. Thereafter, the predicted errors are computed for each possible switching vectors. For each of them, a cost function is evaluated. This cost function (g) provides to the predictive control algorithm the ability of incorporating different objectives. The cost function has been typically defined in MPC as a quadratic measure of the predicted error, which is defined as:

$$\begin{aligned} g &= g_1 + g_2, \\ g_1 &= |I^*_{o\alpha 1} - I_{o\alpha 1}| + |I^*_{o\beta 1} - I_{o\beta 1}|, \\ g_2 &= |I^*_{o\alpha 2} - I_{o\alpha 2}| + |I^*_{o\beta 2} - I_{o\beta 2}|. \end{aligned} \tag{27}$$

From the evaluation of all the possible switching vectors, the algorithm select the optimal switching combination to be applied at the next sampling period.

The proposed control strategy was simulated using Matlab/Simulink simulation environment. System parameters are shown in Table 2. Amplitude reference change responses are shown in Fig. 7. The reference output current was initially set to 20 (A) with a line frequency of 50 (Hz). After t = 0.05 seconds, the amplitude of the reference input current signal was changed and it can be seen that the output current can follow its reference. Moreover, in Fig. 6, the response to a phase change is shown. At t = 0.05 seconds the phase of the reference is changed and the output current can follow its reference with a negligible time constant. In order to compare quantitatively the proposed controller several figures of merit are used, like the mean square error (MSE) and the total harmonic distorsion (THD). The MSE for I_{oa}, I_{ob} and I_{oc} have been quantified at 0.0175, 0.0141 and 0.0149, respectively. At the same time, the THD have been quantified at 5.06 %, 5.19 % and 4.91 %.

5 Conclutions

In this paper a predictive current control technique applied to the MMC architecture for a SpWEG connected to the grid has been proposed and analyzed by simulations. Simulation results have been shown that it is possible to combine the use the advantages of predictive MMC control together with the SpWEG to increase the performance in terms of lower mean squared control error and reliability of the generation system, providing a sinusoidal voltages and currents with low harmonic distortion using fully controlled bi-directional switches without the use of storage energies elements. The multi-modular topology allows to control the supplied current with a negligible error a time constant. Finally, is highlighted that the proposed control technique can be applied for a greater number of modules by setting the correct reference current for each module.

Acknowledgements

The authors would like to thank to the Paraguayan Government for the economical support provided by means of a CONACYT Grant (project 14-INV-097). In addition, they wish to express their gratitude to the anonymous reviewers for their helpful comments and suggestions.

References

[1] N.K. Roy and H.R. Pota, "Current status and issues of concern for the integration of distributed generation into electricity networks," *IEEE Syst. J.*, vol. 9, no. 3, pp. 933–944, Sep. 2015.

[2] A.S. Kumar, and T. Cermak, "A novel method of voltage regulation of isolated six-phase self-excited induction generator fed VSI driven by wind turbine," in *Proc. ICSoEB*, Sousse, Tunisia, 2015, pp. 1–6.

[3] M. Kumawat, N. Gupta, N. Jain, and D. Saxena, "Optimal distributed generation placement in power distributed networks: A review," in *Proc. EESCO*, Visakhapatnam, India, 2015, pp. 1–6.

[4] M. Parvez, S. Mekhilef, N.M.L. Tan, and H. Akagi, "An improved active-front-end rectifier using model predictive control," in *Proc. APEC*, Pasay, Philippines, 2015, pp. 122–127.

[5] D. Sun, B. Ge, W. Liang, H. Abu-Rub, and F. Zheng Peng, "An energy stored quasi-z-source cascade multilevel inverter based photovoltaic power generation system," *IEEE Trans. Ind. Electron.*, vol. 62, no. 9, pp. 5458–5467, Sep. 2015.

[6] P. Acuna, L. Moran, M. Rivera, R. Aguilera, R. Burgos, and V.G. Agelidis, "A single-objective predictive control method for a multivariable single-phase three-level npc converter-based active power filter," *IEEE Trans. Ind. Electron.*, vol. 62, no. 7, pp. 4598–4607, Jul. 2015.

[7] V. Popov, E. Baranov, and A. Malnev, "Current source matrix converter," in *Proc. EDM*, Chemal, Russia, 2015, pp. 384–386.

[8] M. Lopez, J. Rodriguez, C. Silva, and M. Rivera, "Predictive torque control of a multidrive system fed by a dual indirect matrix converter," *IEEE Trans. Ind. Electron.*, vol. 62, no. 5, pp. 2731–2741, May 2015.

[9] C. Garcia, M. Rivera, M. Lopez, J. Rodriguez, R. Pena, P.W. Wheeler, and J.R. Espinoza, "A simple current control strategy for a four-leg indirect matrix converter," *IEEE Trans. Ind. Electron.*, vol. 30, no. 4, pp. 2275–2287, Apr. 2015.

[10] N. Namjoo, F. Abbasi, F. Hassanzadeh, H. Asrari, and A. Hajizadeh, "A new hybrid control method for controlling back-to-back converter in permanent magnet synchronous generator wind turbines" *J. Renew. Sustain. Energy*, vol. 6, pp. 1–13, Jun. 2014.

[11] F. Barrero and M.J. Duran, "Recent advances in the design, modeling and control of multiphase machines – Part 1," *IEEE Trans. Ind. Electron.*, vol. 63, no. 1, pp. 449–458, Jan. 2016.

[12] M. Rivera, A. Wilson, C. Rojas, J. Rodriguez, J. Espinoza, P. Wheeler and Empringham, "A Comparative Assessment of Model Predictive Current Control and Space Vector Modulation in a Direct Matrix Converter" *IEEE Trans. Ind. Electron.* vol. 60, no. 2, pp. 578–588, Feb. 2013.